Paper No.
PPU13

Microstrutural Characterisation and Corrosion Behaviour of 9Cr–1Mo Steel Based Metal Waste Form Alloys with Noble Metal Fission Products

R. Priya

Corrosion Science and Technology Division
Indira Gandhi Centre for Atomic Research, Kalpakkam - 603102, India.
rpriya@igcar.gov.in

S. Ningshen, C. Mallika and U. Kamachi Mudali

Corrosion Science and Technology Division
Materials Chemistry and Metal Fuel Cycle Group
Indira Gandhi Centre for Atomic Research, Kalpakkam - 603102, India.

ABSTRACT

Pyrochemical reprocessing technique based on electro-refining process is proposed for the extraction of uranium and plutonium from the spent metallic fuels, which would be discharged from future Fast Breeder Reactors (FBRs) in India. In electro-refining, the noble metal fission products (NMFPs), steel cladding hulls and zirconium from the alloy fuel that are not oxidized, remain in the anode basket as metallic waste. The solid metallic waste in the anode dissolution basket of the electro-refiner along with contaminated actinide elements is consolidated by melting to produce Metal Waste Form (MWF) alloys for disposal in geological repositories. The waste matrix to be produced for immobilizing the radioactive waste must possess excellent chemical stability and durability, besides its compatibility with the waste stream as well as the disposal environment. In the present work, the influence of NMFPs on the microstructure and corrosion behavior of 9Cr1Mo steel-12Zr MWF alloys in simulated ground water media was studied. Ingots of 9Cr1Mo steel-12Zr-NMFPs MWF alloy with different NMFP concentrations (1-4 wt.%) were prepared by vacuum arc melting. The XRD pattern of the MWF alloy showed the presence of α-Fe peak and the intermetallics phases $Fe_{23}Zr_6$, and Fe_2Zr. The noble metal fission product intermetallics were found in 2.5 NMFP and 4 NFFP MWF alloys. Potentiodynamic polarization behavior showed improved corrosion resistance for 2.5 NMFP and 4 NMFP alloys than in 1 NMFP MWF alloy in simulated Rajasthan Ground Water (RGW) and Kalpakkam Ground Water (KGW) media. Electrochemical impedance spectroscopy (EIS) results revealed higher passive film stability for 2.5 NMFP and 4 NMFP MWF alloy in RGW and KGW media. Higher breakdown potential and polarization resistance values were observed in RGW than in KGW medium. Corrosion morphology showed more pits and corrosion attack at KGW than in RGW medium. The concentration of the NMFP played an important role in improving the corrosion resistance of the MWF alloy.

Keywords: Noble metal, Intermetallics, Polarization, Impedance and Passive film

INTRODUCTION

Pyrochemical reprocessing of spent metallic fuels from fast breeder reactors results in the generation of metal nuclear waste. Consolidating the solid metal waste along with other liquid wastes into a borosilicate glass matrix is technically difficult and hence, needed a separate treatment. Metal waste Form (MWF) alloy based on 9Cr1Mo steel with Zr is proposed for the disposal of solid waste generated from the pyro-reprocessing of metallic spent fuels of commercial fast breeder reactors, because of its beneficial properties over D9 stainless steel that shows better resistance to void swelling, low thermal expansion coefficient and high thermal conductivity. The waste comprising the cladding hull left over in the anode basket after dissolution of the spent fuel and electro-refining step, noble metal fission products (Tc, Ru, Rh, Pd), Nb, actinides and zirconium metal from the metallic alloy fuel are consolidated by melting at 1600°C to form Fe-Cr-Zr MWF alloys[1-6]. Corrosion is an important phenomenon, which must be taken into serious account considering the integrity of the metal waste form alloys in geological repository. Previously the corrosion behavior of D9 SS based MWF alloys was studied in detail and and the metal waste form alloys with 8-12 wt% Zr content has the best passive film stability and higher corrosion resistance[7]. From the elaborated studies of D9 SS based MWF alloys, it is shown that the MWF alloy exhibited appreciable corrosion resistance and selective leaching of elements due to the presence of Fe-Zr rich intermetallics and these phases acted as the hosting phases for the noble metal fission products and actinides[7-9]. Polarization studies of 304 stainless steel-based metal waste form shows passive behavior in all solutions (all pH and chloride environments)[10]. Impedance measurements indicate passivity breakdown events leading to localized corrosion in alkaline conditions. Hence, the localized corrosion can be expected in stainless steel based metal waste form alloys in alkaline environment and uniform dissolution in acidic conditions. In the present work, the development of Fe-9Cr-1Mo-Zr MWF alloys and the influence of noble metal fission products (NMFPs) on the microstructure and corrosion behavior in simulated ground water media are focused and briefly highlighted.

EXPERIMENTAL PROCEDURE

ALLOY MELTING AND SAMPLE PREPARATION

Ingots of MWF alloys have been prepared with alloy 9Cr-1Mo stainless steel - 12 wt.% Zr with different weight percent of noble metal fission products. The ingots required for this study was prepared by vacuum arc melting furnace. The alloy was melted six times for better homogeneity in high purity inert argon gas atmosphere. The melt was allowed to cool inside the furnace to obtain rectangular shaped cast form. Alloys prepared by the above method were cut into pieces and then ground in SiC paper on all sides. These specimens were then mounted in an epoxy resin with a brass rod for electrical connection. The exposed surfaces of the mounted specimens were ground to 1200 grit SiC emery paper and then polished up to 1µm diamond finish for corrosion studies. Special precautions were taken to ensure that crevice corrosion at the edges of the samples-mount interface did not occur. The edges of the sample were covered by corrosion resistant lacquer that will prevent the crevice attack at sample-mount interface.

MICROSTRUCTURAL CHARACTERIZATION

The detailed microstructural study of MWF alloys were carried out by scanning electron microscope (SEM) in back scattered electron (BSE) mode. The MWF alloy specimens have been etched by Villella's reagent (1g picric acid + 5ml Hydrochloric acid + 100ml of ethyl alcohol) for 15s to reveal the microstructure. The lattice phases present in these MWF alloys have been studied by X-ray diffraction. Powder XRD system used is of the model INEL EQUINOX 2000. The X-ray source used is Co-Kα. X-ray diffraction (XRD) data were collected and the data has been analyzed with the help of JCPDS software.

ELECTROCHEMICAL CHARACTERIZATION

Open Circuit Potential and Potentiodynamic Polarization

The potentiodynamic anodic polarization studies to evaluate the corrosion resistance properties of MWF alloys were carried out in simulated Rajasthan round water (RGW) and Kalpakkam ground water (KGW) prepared in de-mineralized water by the addition of respective chemical salts. All the potentiodynamic polarization experiments were carried out at room temperature using the five neck ASTM electrochemical cell consisting of three electrodes system; reference electrode (Ag/AgCl – in saturated KCL), counter electrode (Pt) and working electrode (specimen). The electrochemical interface was used for the polarization experiments. The potentiodynamic polarization is performed at the scan rate of 0.166 mV/ min and the polarization was continued until the transpassive potential occurred. Three sets of tests were conducted for each specimen and all the polarization plots were almost reproducible.

Electrochemical Impedance Spectroscopy

Electrochemical impedance spectroscopy (EIS) measurements were carried out using frequency response analyzer (FRA) and an electrochemical interface. The experiments were conducted in the frequency range 0.01 - 10^5 Hz by superimposing an AC voltage of 10 mV amplitude at open circuit potential in simulated Rajasthan and Kalpakkam ground water. The results were interpreted using single time constant equivalent circuit.

RESULTS

MWF alloy	Ru	Rh	Pd
1-NMFP	0.46	0.16	0.31
2.5-NMFP	1.3	0.47	0.8
4-NMFP	2.0	0.7	1.2

Table 1 Chemical composition of Ru, Rh and Pd in wt.%

INGOT CHEMICAL COMPOSITION ANALYSIS

The typical as cast ingot picture is shown in Figure 1. The chemical composition analysis of Ru, Rh and Pd present in the ingot was analyzed by Induction coupled plasma optical emission spectroscopy (ICP-OES) and it is listed as wt. % in Table 1 for the three different 9Cr1Mo steel-12Zr-NMFPs MWF alloys. . The concentrations of the noble metal fission products determined by ICP method are given in Table 1.

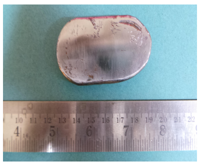

Figure 1 Typical as cast ingot (9Cr1Mo-12Zr-4 NMFP) MWF alloy

SEM AND XRD ANALYSIS

The SEM-BSE image of the 9Cr1Mo steel-12Zr-NMFPs MWF alloys is shown in Figure 2. The microstructure revealed two different contrasts of bright and dark lamellar structure. Similar microstructural features were observed for the three MWF alloys. The addition of Zr to 9Cr1Mo steel resulted in the formation of intermetallic phases as Zr has a very low solubility in Fe. Simultaneous formation of α-Fe and Fe-Zr intermetallic phases resulted in a layered eutectic microstructure. The dark region corresponds to Fe based solid solution phase, and the bright contrast region to Zr enriched phase. The XRD pattern of 9Cr1Mo steel-12Zr-NMFP based MWF alloys are shown in Figure 3. Phase characterization revealed the presence of α- Fe, Fe_2Zr and $Fe_{23}Zr_6$ stable phases. The noble metal fission products are also present in the solid solution. MWF alloys show the intermetallic peak intensity is comparatively weaker for 1 NMFP than 2.5 NMFP and 4 NMFP MWF alloy. The relative intensity of the intermetallic peak intensity increases with the increase in NMFPs. NMFP intermetallics (FeRu, Fe_3Rh_7 and $FePd_3$) are also observed along with Fe-Zr intermetallics for

2.5 NMFP and 4 NMFP MWF alloy. However, the NMFP intermetallic in 1 NMFP MWF alloy is below the detection limit and only FeRu is observed along with Fe_2Zr phase.

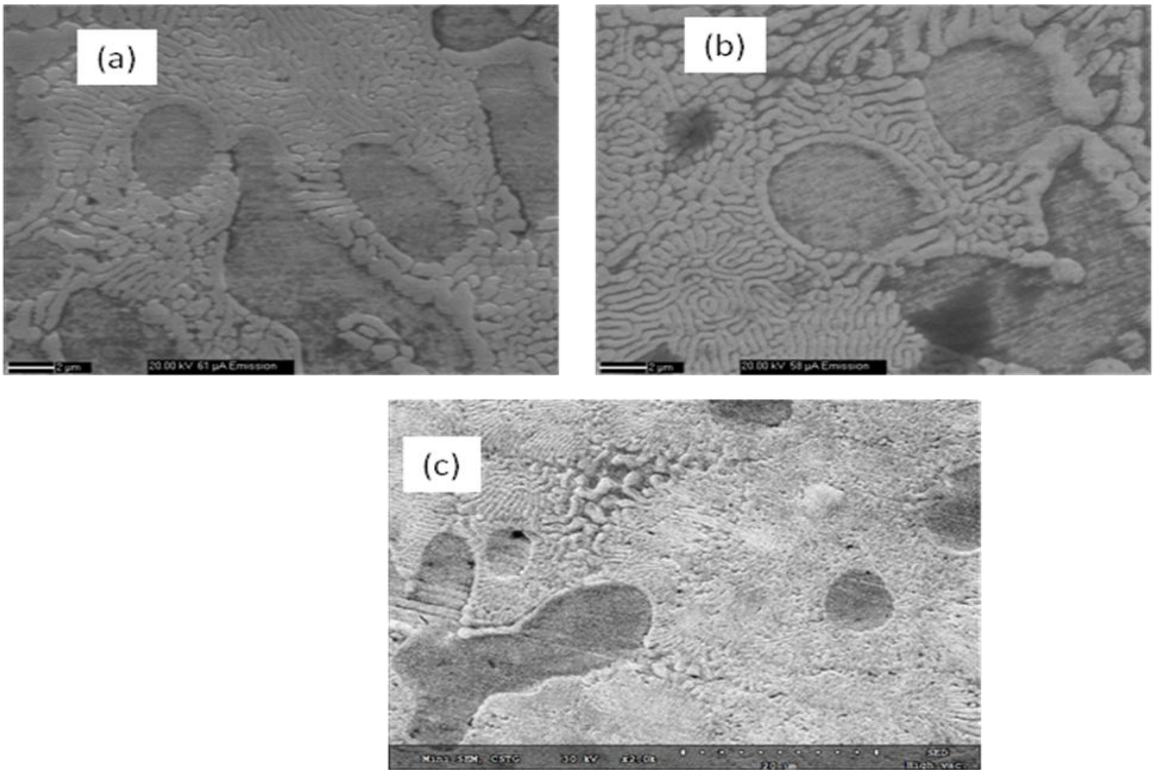

Figure 2: SEM – BSE images of the 9Cr1Mo steel-12Zr-NMFP MWF alloys a) 1 NMFP 2) 2.5NMFP and 3) 4NMFP

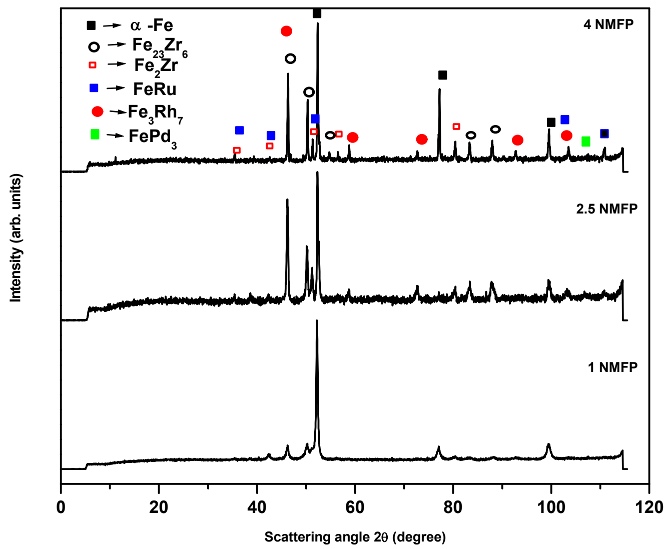

Figure 3: XRD pattern of the 9Cr1Mo steel-12Zr-NMFP MWF alloys

ELECTROCHEMICAL CHARACTERIZATION

OCP

The open circuit potential (OCP)-time plots of 9Cr1Mo steel-12Zr-NMFP MWF alloys measured at RGW and KGW are shown in Figure 4a and 4b respectively. The steady state OCP was observed in RGW medium. The OCP behavior in RGW was similar for the tested alloys irrespective of the NMFP contents. However, the OCP behavior was nobler for 2.5 NMFP and 4 NMFP than 1NMFP MWF alloy. Thus the increase in NMFP concentration has shifted the OCP nobler.

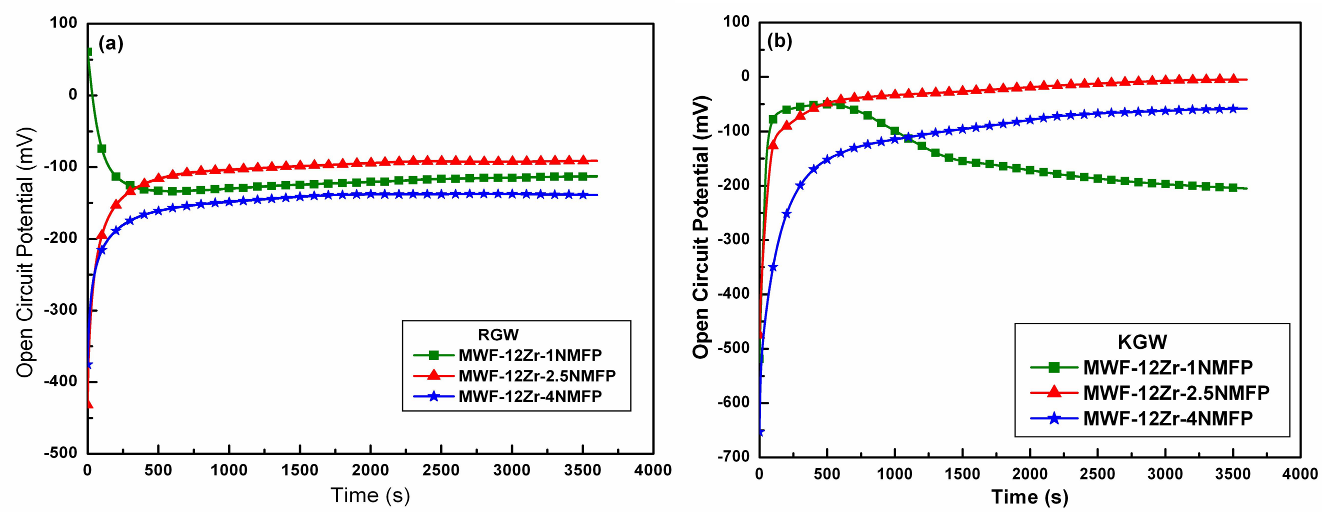

Figure 4: OCP behavior of the 9Cr1Mo steel-12Zr-NMFP MWF alloys (a) RGW and (b)KGW

POTENTIODYNAMIC POLARIZATION

The potentiodynamic polarization behavior plots of 9Cr1Mo steel-12Zr-NMFP MWF alloys at RGW and KGW media are shown in Figure 5a and 5b respectively. In both RGW and KGW media, the corrosion potential is higher for 2.5 NMFP and 4 NMFP MWF alloys than 1 NMFP MWF alloy. The

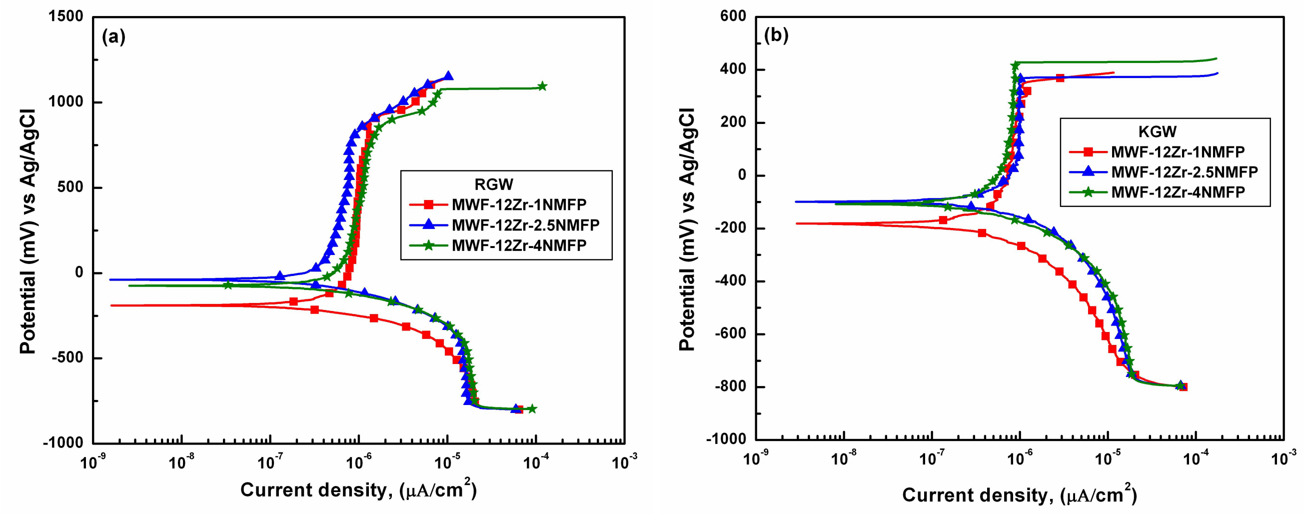

Figure 5: Potentiodynamic polarization behaviour of the 9Cr1Mo steel-12Zr-NMFP MWF alloys (a) RGW and (b)KGW

Increased corrosion potential in 2.5 NMFP and 4 NMFP MWF alloy is attributed to the more stable passive film formation with increase in noble metal concentration of the alloy. Higher breakdown potential was observed for the alloys in RGW (~1000 mV) than in KGW medium (~400 mV). This is due to the higher Cl^- ion concentration in the KGW that lead to easy breakdown of the passive film when compared to RGW medium.

EIS

The electrochemical impedance spectroscopy (EIS) measurement of 9Cr1Mo steel-12Zr-NMFPs MWF alloy in RGW and KGW media at open circuit potential (OCP) conditions are shown in Figure 6a and 6b, respectively. The Nyquist plot showed that the impedance arc diameter increases with increase in NMFP concentration of the MWF alloys. The EIS results of RGW indicated that the polarization resistance is higher for 2.5 NMFP and 4 NMFP MWF than 1 NMFP MWF alloy. In the chloride rich KGW medium, the 4 NMFP MWF alloy exhibited a higher polarization resistance and lower capacitance when compared to 2.5 NMFP and 1 NMFP MWF alloys. Thereby, indicating that the passive film stability is influenced by the concentration of NMFPs in MWF alloys. Higher passive film stability is observed in RGW than KGW medium. The polarization resistance (R_p) is one order of magnitude higher in RGW than KGW. This is attributed to the fact that higher concentration of Cl^- ion in KGW media lowered the passive film stability whereas the lower concentration of Cl^- ion in RGW had favored the formation of hydrated passive film especially the insoluble (Ca and Mg) SO_4 layer.

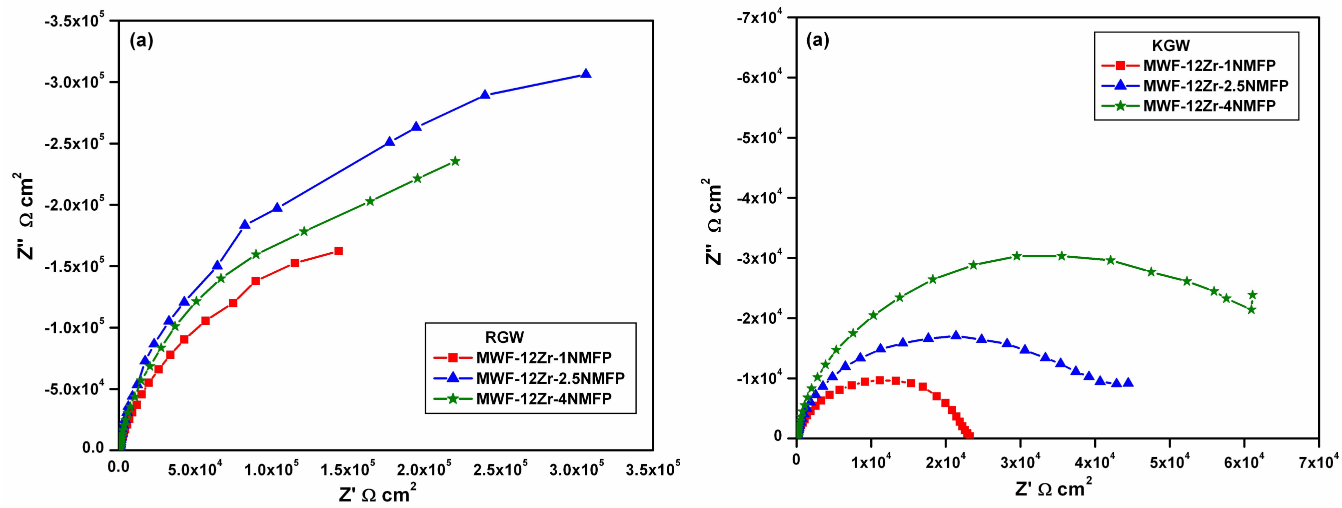

Figure 6: Nyquist plot of 9Cr1Mo steel-12Zr-NMFP MWF alloys (a) RGW and (b) KGW

The passive film stability is largely influenced by the presence of NMFP concentrations and has influence on the corrosion resistance of the MWF alloy. Thus, 2.5 NMFP and 4 NMFP MWF alloys shows better corrosion resistance in the tested geological repository media.

CONCLUSIONS

Successful melting of Fe-9Cr-1Mo-Zr MWF alloys with different concentration of NMFP was achieved and the concentration of NMFP plays a significant role in the formation of intermetallics that affected the corrosion resistance of the MWF alloys. The microstructure of the 9Cr1Mo steel-12Zr-(1-4 wt.%) NMFP MWF alloys showed eutectic lamellar structure. The XRD analysis revealed the presence of stable phases of α-Fe, Fe_2Zr, $Fe_{23}Zr_6$, FeRu and Fe_3Rh_7. The NMFP intermetallics are observed only for the MWF alloy with 2.5 and 4 NMFP and the peak intensity increased with increase in NMFP concentrations. Improved corrosion resistance was observed for 2.5 NMFP and 4 NMFP alloys than 1 NMFP MWF alloy in both RGW and KGW medium. Electrochemical impedance spectroscopy (EIS) results revealed higher passive film stability for 2.5 NMFP and 4 NMFP MWF alloy in RGW and KGW media respectively. The corrosion resistance of the MWF alloys is greater in RGW than in KGW medium.

REFERENCES

1. D. D. Keiser Jr. and S. M. McDeavitt, "Actinide-Containing Metal Disposition Alloys, Proc. DOE Spent Nuclear Fuel & Fissile Material Management", Reno, Nevada, June 16-20, 1996, American Nuclear Society, LaGrange Park, Illinois (1996).

2. S.M. McDeavitt, J.Y. Park and J.P. Ackerman, "Defining a metal-based waste form for IFR pyroprocessing wastes, Actinide Processing: Methods and Materials", eds. B. Mishra and W.A. Averill, Minerals, Metals & Materials Society, Warendale, Pennsylvania (1994) pp. 305-319.

3. D.P. Abraham and S.M. McDeavitt, J.Y. Park, "Microstructure and phase identification in type 304 stainless steel-zirconium alloys", Metall. Mater. Trans. 27A (1996) pp. 2151-2159.

4. D.E. Janney, "Host phases for actinides in simulated metallic waste form", J. Nucl. Mater. 323 (2003) pp. 81-92.

5. D.P. Abraham, J.W. Richardson and S.M. McDeavitt, "Laves intermetallics in stainless steel-zirconium alloys", Mater. Sci. Eng. A. 239-240 (1997) pp. 658-664.

6. D.P. Abraham, N. Dietz, "Role of laves intermetallics in nuclear waste disposal", Mater. Sci. Eng. A. 329-331(2002) pp. 610-615.

7. L.R. Bairi, S. Ningshen, U. Kamachi Mudali and Baldev Raj, "Microstructural analysis and corrosion behavior of D9 stainless steel – zirconium metal waste form alloys", Corros. Sci. 52 (2010) pp. 2291-2302.

8. L.R. Bairi, S. Ningshen, U. Kamachi Mudali and Baldev Raj, "Corrosion issues related to disposal of 316 SS-zirconium metal waste form under simulated repository conditions", Corros. Eng. Sci. Technol. 146 (2011) pp. 171-176.

9. L.R. Bairi, C. Mallika and U. Kamachi Mudali. , "Influence of noble metal fission products and uranium on the microstructure and corrosion behaviour of D9 Stainless Steel – Zirconium metal waste form alloy", J. Nucl. Mat. 448 (2014) pp. 340-347.

10. N. Das, P. Sengupta, S. Roychowdhury, G. Sharma, P.S. Gawde, A. Arya, V. Kain, U.D. Kulkarni, J.K. Chakravartty, G.K. Dey, Metallurgical characterizations of Fe-Cr-Ni-Zr base alloys developed for geological disposal of radioactive hulls, J. Nucl. Mat. 420 (2012) pp. 559-574.